Macromolecules
ARTICLE

Macromolecules **2011**, *44*, 39–45 **39**
DOI: 10.1021/ma102438k

High Ionic Liquid Content Polymeric Gel Membranes: Preparation and Performance

Johannes Carolus Jansen*

Institute on Membrane Technology, ITM-CNR, c/o University of Calabria, Via P. Bucci 17/C, 87030 Rende (CS), Italy

Karel Friess

Institute of Chemical Technology Prague, Department of Physical Chemistry, Technická 5, Prague 6-Dejvice, 166 28 Czech Republic

Gabriele Clarizia

Institute on Membrane Technology, ITM-CNR, c/o University of Calabria, Via P. Bucci 17/C, 87030 Rende (CS), Italy

Jan Schauer

Institute of Macromolecular Chemistry, Heyrovského nám. 2, 162 06 Prague 6-Břevnov, Czech Republic

Pavel Izák

Institute of Chemical Process Fundamentals, Rozvojová 135, 165 02 Prague 6-Suchdol, Czech Republic

Received October 25, 2010; Revised Manuscript Received December 2, 2010

ABSTRACT: Ionic liquid polymeric gel membranes containing from 20 wt % to 80 wt % of the ionic liquid 1-ethyl-3-methylimidazolium bis(trifluoromethylsulfonyl)imide ([EMIM][TFSI]) in poly(vinylidene fluoride-*co*-hexafluoropropylene) (p(VDF-HFP)) were prepared by solvent casting from a solution in acetone. The effect of the ionic liquid on the performance and properties of the membranes was discussed and compared with the neat polymer. In the presence of an excess of ionic liquid, p(VDF-HFP) membranes swell in a significant way, especially above 70 °C, becoming completely soluble above 90 °C. DSC analysis shows a gradual decrease of the melting point of the gel and a decrease in the overall melting enthalpy with increasing IL content, whereas the melting enthalpy normalized for the polymer fraction shows an initial drop and then a gradual increase. In the presence of the ionic liquid, the elastic modulus and break strength decrease dramatically, while the maximum deformation first increases due to higher flexibility of the plasticized polymer and then rapidly decreases above 40 wt % of IL as a consequence of the progressive decrease of the number of entanglements. X-ray studies demonstrate a reduction in the overall crystal content. The position of the strongest diffraction peak remains unaltered in all samples, suggesting that only the polymer chains crystallize and that no cocrystallization of ionic liquid and polymer takes place. Preliminary gas permeation measurements show a significant increase of the permeability in the presence of [EMIM][TFSI], especially for carbon dioxide. This suggests a potential application in gas separation membranes, for instance for natural gas treatment or for CO_2 sequestration from flue gas.

Introduction

During the past few years, ionic liquids (IL) have been recognized as a possible environmentally benign alternative to the classical organic solvents, mainly due to their good thermal stability and ability to dissolve a large range of organic molecules.[1] Ionic liquids have also been successfully applied in a wide range of applications, for instance in asymmetric synthesis, electrochemical applications, extractive separation in biotechnology,[2−4] and also in membrane gas separations[5] and pervaporation.[6] Their successful use is based on their extremely low volatility and consequent stability of the membrane compared to traditional supported liquid membranes.

*Corresponding author. E-mail: jc.jansen@itm.cnr.it.

Ionic liquid membranes are usually prepared in the form of supported liquid membranes, in which the pores of a porous membrane are saturated with the room temperature ionic liquid (RTIL).[7] In such membranes, the ionic liquid is trapped inside the pores by capillary forces. Although evaporation of IL can be excluded, if such membranes come in contact with a liquid phase, for instance in pervaporation, they can loose the ionic liquid from inside the polymer network due to swelling and leaching into the liquid phase.

To avoid this problem, in other cases membranes were prepared from polymerized room-temperature ionic liquids.[8,9] These RTILs are more stable but they require particular polymerizable groups and sophisticated membrane preparation techniques.

Published on Web 12/14/2010

IL Gels/Membrane Preparation and Their Use. Numerous polymers may form thermoreversible gels from dilute or concentrated solution in the proper solvent.[10] A continuous physical network structure extending throughout the volume of the system is formed when at a certain reduced solvent power of the medium the polymeric chains form association complexes at widely separated points. In the majority of the cases these gels derive from the existence of a crystalline network structure, formed upon cooling from the homogeneous solution.

Such gels may also be formed starting from the polymer solution in a solvent mixture, in which "the good solvent" is allowed to evaporate and the second poor solvent is nonvolatile. Upon evaporation of "the good solvent", the polymer will phase separate. Under the proper conditions, and if the polymer is far enough below its nominal melting temperature, phase separation may take place as solid−liquid demixing. In this case, the free energy minimization favors the formation of small crystals as a solid phase in the liquid mixture. In this process, the polymer chains in solution form bridges between different crystals, diminishing chain mobility so much as to preclude subsequent macroscopic phase separation. In other cases the crystallization may be preceded by liquid−liquid phase separation, if a poor solvent or a solvent mixture is used and the process takes place not too far below the polymer melting point.

Very few cases have been reported where the thermoreversible gels are based on ILs as the poor solvent for the polymer. Recently Harner and Hoagland reported thermoreversible poly(ethylene glycol)/1-ethyl-3-methylimidazolium ethylsulfate [EMIM][$EtSO_4$] ionic liquid gels.[11] He and Lodge reported gels of 1-ethyl-3-methylimidazolium bis(trifluoromethylsulfonyl)imide [EMIM][TFSI] in acrylamide and ethylene oxide-based triblock or pentablock copolymers.[12] Kawauchi et al. reported thermoreversible ion gels based on poly(methyl methacrylate)s in 1-butyl-3-methylbenzimidazolium hexafluorophosphate.[13]

The supported liquid membranes have been tested for targeted gas/gas separations and especially for separation from air of volatile organic compounds,[14,15] leaking from gasoline during its storage, transportation and handling. In comparison with frequently used polymers like polydimethylsiloxane (PDMS),[16−18] polyether−polyamide block copolymer (PEBA), poly(vinylidene fluoride) (PVDF), high-free volume amorphous glassy perfluoropolymers,[19] or cross-linked fluorinated or poly(amide-imide) polymers,[20,21] RTIL supported membranes are, highly absorbing for alkanes and aromates without enormous material swelling. They also provide higher mass fluxes of separated substances or high separation factors.[22]

Scope. The aim of the present work is to develop, using a simple solution casting technique, stable RTIL membranes in which the IL is trapped inside a polymer gel phase. A further aim is to gain insight into the thermal, mechanical and structural properties of the gel phase and their correlation with the transport properties, in view of the potential use of such membranes in gas separation processes.

Experimental Part

Materials. Acetone (analytical grade, Lachner, Czech Republic) and ionic liquid 1-ethyl-3-methylimidazolium bis(trifluoromethylsulfonyl)imide (puriss., 99%, Solvent Innovation, mp −20 °C) were used without further purification. The ionic liquid (see Figure 1) will further be abbreviated as [EMIM][TFSI].

Poly(vinylidene fluoride-*co*-hexafluoropropylene) *fluoroelastomer*, further abbreviated as p(VDF-HFP), with nominal M_n = 130 000 g/mol, M_w = 400 000 g/mol, melting point 140−145 °C and molecular structure $-[CH_2-CF_2]_n-[CF_2-CF(CF_3)]_m-$ was supplied by Sigma-Aldrich.

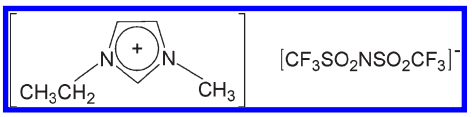

Figure 1. Structure of the ionic liquid 1-ethyl-3-methylimidazolium bis(trifluoromethylsulfonyl)imide ([EMIM][TFSI]).

The gases for the permeation tests (nitrogen, oxygen, methane, helium, hydrogen, and carbon dioxide, all with purity 99.99+%) were supplied by Pirossigeno, Italy.

Membrane Preparation. The polymer solution was prepared by dissolving 10 wt % of p(VDF-HFP) in acetone at room temperature under magnetic stirring for at least 1 h until a clear homogeneous solution was obtained. Different amounts of the ionic liquid [EMIM][TFSI] were added to the polymer solution under magnetic stirring and they dissolved completely in a few minutes.

The membranes were prepared by solution casting of the polymer/ionic liquid mixture in acetone on a Petri dish and by subsequent solvent evaporation at room temperature for 24 h. The membranes were further dried at 70 °C for 4 h to guarantee complete removal of the volatile solvent.

Membrane Swelling and Solubility Tests in [EMIM][TFSI]. Films of pure p(VDF-HFP) with a thickness of 0.15 mm were dried under vacuum at 80 °C, weighed, and immersed in an excess of pure [EMIM][TFSI] ionic liquid. After 48 h the films were removed from the liquid, wiped with tissue paper, and weighed again to determine the amount of ionic liquid absorbed. The experiments were carried out at different temperatures from 25 to 85 °C.

DSC. The thermal properties of the membranes were determined by DSC analysis, using a Pyris Diamond differential scanning calorimeter (Perkin-Elmer) equipped with Intracooler refrigeration system. Samples of 10−16 mg were wrapped in a small disk of aluminum foil (< 5 mg) and were subjected to a heating/cooling/heating cycle in the range from −50 to +200 °C at a rate of 20 °C/min. Given the low weight of the sample holder, no reference was used. Baseline subtraction was used to reduce the curvature of the baseline. The temperature and heat flow were calibrated with indium and zinc standards.

Mechanical Properties. Tensile tests on the membranes were carried out at room temperature on a Zwick/Roell single column Universal Testing Machine, model Z2.5, equipped with a 50 N load cell and flat pneumatic clamps. The clamp surface was covered with adhesive rubber to avoid slipping or damage of the softer samples with high IL content.

Specimens with an effective length of 40 mm (distance between the clamps) and a width of 5 mm were tested at a deformation rate of 20 mm min^{-1} (= 50% min^{-1}), with exception of the sample without IL, which was tested at a deformation rate of 8 mm min^{-1} (= 20% min^{-1}) to avoid early rupture due to its higher stiffness and fragility. The average value and the standard deviation of the Young's modulus, the break strength and the maximum deformation were determined on a series of 4−6 samples.

X-ray. The XRD data of sample films (20 × 15 mm) were collected at room temperature by an X'Pert PRO $\theta-\theta$ diffractometer (PANanalytical, The Netherlands) using Cu Kα radiation (λ = 1.5418 Å, U = 40 kV, I = 30 mA) in parafocusing Bragg−Brentano geometry. The data were scanned with an ultrafast X'Celerator detector over the angular range 5−70° (2θ) with a step size of 0.033° (2θ) and time per step 20.32 s. Data evaluation was performed by the software package HighScore Plus.

Gas Permeability Measurements. Gas permeation rate tests on flat dense membranes were carried out at room temperature (25 °C) by fixed-volume pressure increase instrument, described in detail elsewhere.[23] After thorough evacuation of the membrane

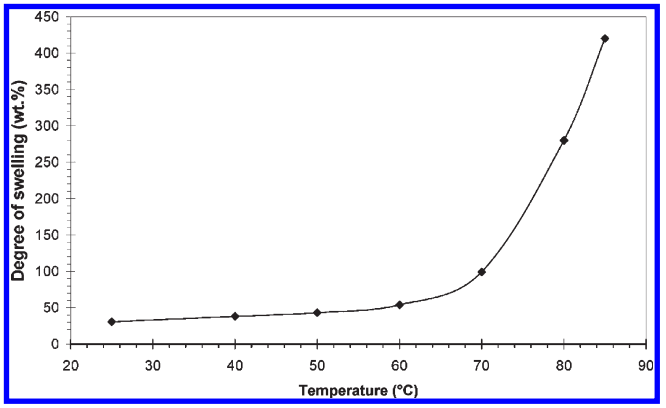

Figure 2. Temperature dependence of the swelling degree of the p(VDF-HFP) fluoroelastomer in excess ionic liquid [EMIM][TFSI].

to remove all previously dissolved species, the membrane is exposed to the feed gas and from that moment the pressure in the fixed permeate volume is monitored. Measurements were carried out with six permanent gases (He, H_2, CH_4, N_2, O_2, and CO_2). Permeability coefficients, P, were calculated from the slope of time-pressure curve in steady state condition:[24]

$$p_t = p_0 + (\mathrm{d}p/\mathrm{d}t)_0 t + \frac{RTA}{V_p V_m}\frac{p_f P}{l} t \qquad (1)$$

in which p_t is the permeate pressure at time t, p_0 is the starting pressure, $(\mathrm{d}p/\mathrm{d}t)_0$ is the baseline slope. R is the universal gas constant, T is the absolute temperature, A is the exposed membrane area, V_P is the permeate volume, V_m is the molar volume of a gas at standard temperature and pressure [0 °C and 1 atm], and p_f is the feed pressure. The transport properties of the gases were determined at the feed pressure of 1 bar. A total membrane area of 11.3 or 34.2 cm^2 was used.

Results and Discussion

Membrane Preparation. All membranes in this work were cast from solutions in acetone, a good common solvent for both the fluoroelastomer and the ionic liquid [EMIM][TFSI]. The membranes were prepared by controlled solvent evaporation. As a result of the evaporation of acetone ("the good solvent") the relative concentration of IL ("the less good solvent") and polymer increased. In this way, the deteriorating solvent quality leads to gelation of the solution by crystallization of the polymer and to the gradual formation of a solid film. Upon complete drying at higher temperature, mechanically resistant transparent self-supported membranes were obtained for all ratios of polymer and ionic liquid. Often a small amount of IL exudate appeared on the surface of the membranes as tiny droplets or as a thin film.

Membrane Swelling and Solubility Tests in [EMIM][TFSI]. Swelling of pure p(VDF-HFP) films in excess IL was carried out at different temperatures. The degree of swelling (DS) of the neat polymer films after 48 h was calculated using the relationship:

$$\mathrm{DS} = (W_S - W_0)/W_0 \qquad (2)$$

where W_S is the weight of the swollen sample and W_0 is the weight of the same film before immersion.

It was found that at room temperature (25 °C) the neat p(VDF-HFP) film swells about 30 wt % in [EMIM][TFSI]. The swelling increases more or less linearly with temperature up to about 60 °C and then increases dramatically above 70 °C (Figure 2). Above 90 °C, the polymer becomes completely

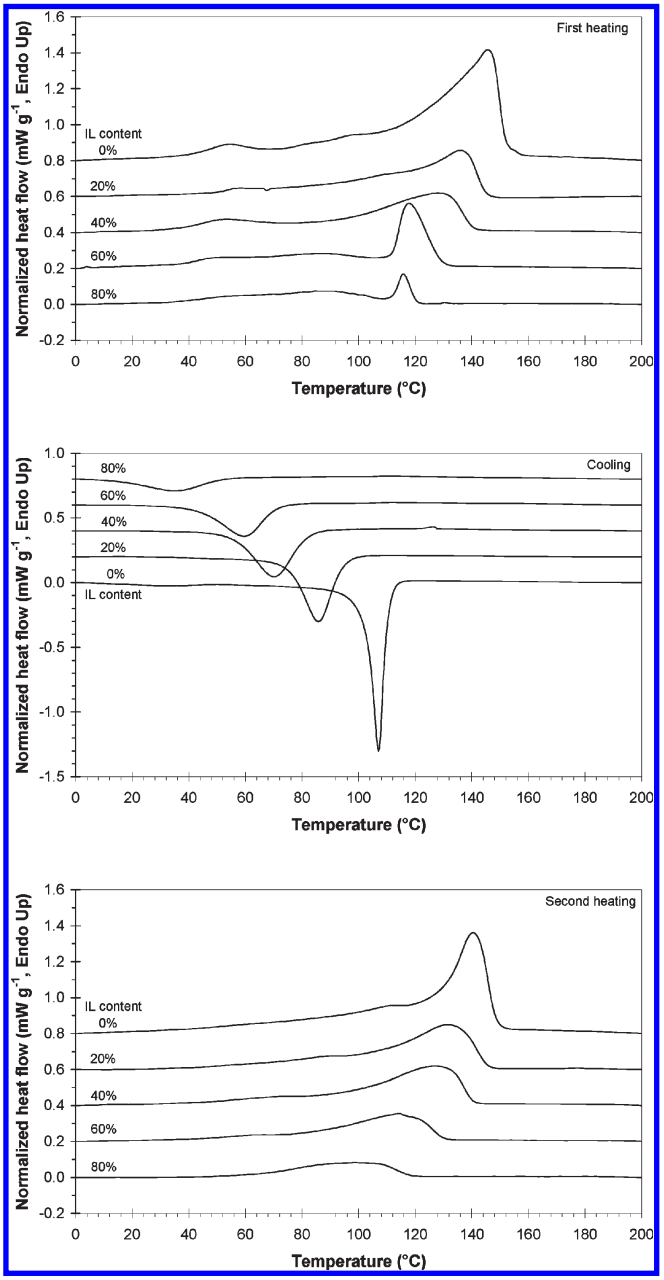

Figure 3. DSC thermograms of the freshly prepared samples during heating (top), the successive cooling run (middle), and the second heating run (bottom). Curves are shifted vertically for clarity.

soluble. Once dissolved, the polymer remains in solution even upon cooling down to room temperature. This behavior confirms the good compatibility of the polymer with the ionic liquid. The complete dissolution of the polymer above 90 °C is in accordance with the strong melting point depression of the membranes with the highest IL content observed by DSC analysis. Obviously the melting of the crystalline phase of the polymer corresponds with the point where the polymer becomes soluble. In this light, swelling of a neat polymer film in the IL could be a successful alternative method to prepare IL-containing membranes. However, this is not suitable to reach high IL concentrations because the membrane is easily deformed or damaged during the swelling as a result of the dissolution and extraction of the low molar mass fraction of the polymer.

Thermal Analysis of the Gel Membranes. The thermal properties of the membranes were investigated by DSC

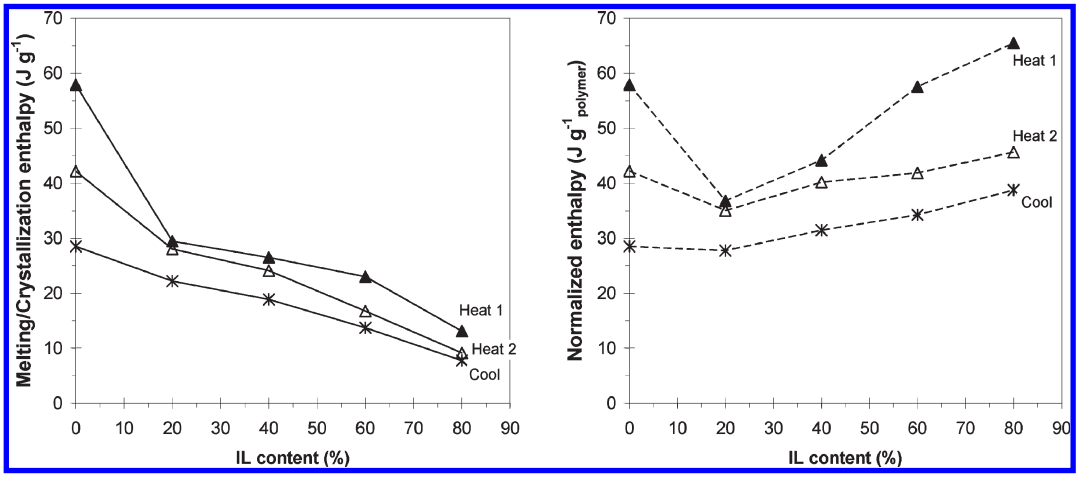

Figure 4. Total melting and crystallization enthalpy of the overall membranes (left) and after normalization for the polymer content (right). Heat 1, Heat 2, and Cool indicate the first and second heating run and the cooling run, respectively.

analysis. The results are displayed in Figure 3. With increasing IL content there is a strong decrease of the melting temperature of the gel in comparison with the pure polymer. At the same time the strong and relatively sharp peak makes place for a much weaker and broader melting peak, suggesting a reduction of the average crystal size and/or purity. The differences in the melting and crystallization peak temperature are related to the kinetics of the crystallization process. In the present case the degree of supercooling depends on the viscosity of the system (related among others to the molar mass, chain flexibility and polymer concentration) and on the probability that polymer chains approach one another to form a stable nucleus (related again to the polymer concentration in the ionic liquid).

Up to 80% of IL in the membrane the gelation is thermally reversible above room temperature, as can be seen from the strong endothermal crystallization peak in the cooling curves. Both the crystallization temperature and the enthalpy decrease markedly with increasing IL content.

The stable solution obtained during the swelling and solubility tests of the polymer in the IL is apparently only possible at very low polymer concentrations. The dissolution temperature of 90 °C observed in the swelling tests in excess IL corresponds approximately to the melting point of the gels, if we extrapolate the data from Figure 3 to higher IL content and to lower polymer concentration.

Given the thermal reversibility of the gel formation also the thermally induced phase separation process (TIPS) should in principle be a possible alternative for the current solution-casting membrane formation process. Nevertheless, from the viewpoint of practical applicability the solution casting is the better process because it is easier to obtain thin films, thus limiting the consumption of expensive ionic liquid.

The overall melting enthalpy of the films decreases almost linearly with increasing IL content, obviously due to the lower polymer concentration (Figure 4). However, if this value is normalized for the polymer concentration, a different trend is found: after an initial decrease, going from neat polymer to 20 wt % of IL, with a further increase of the IL content the normalized melting enthalpy also slightly increases. This is even more evident in the freshly prepared sample, in which crystallization has taken place during evaporation of the solvent, and it is an indication that crystallization is more efficient due to higher freedom of motion of single chains in the diluted phase. The measured crystallization enthalpy is somewhat lower than the melting enthalpy

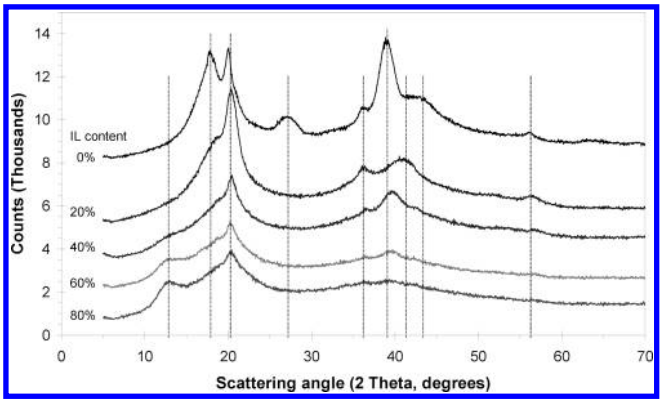

Figure 5. Wide-angle X-ray diffraction patterns of the membrane samples (*x*-axis °2θ, *y*-axis counts or arbitrary units). The lines are shifted vertically for better comparison.

in the second run. This indicates that at the given cooling rate of 20 °C/min crystallization is not totally complete in the measurement window shown in Figure 3. Evidently some further crystallization takes place when the sample is cooled to −50 °C before the next measurement.

In this light it is interesting to note that the samples with 60 and 80 wt % IL show a quite unique and remarkably sharp melting peak just below 120 °C in the fresh sample. In the case of PVDF, which has different crystal polymorphs, it is known that in solution-cast films the type of solvent can influence which polymorph will be formed predominantly,[25] Also in the present p(VDF-HFP) copolymer we believe that mainly the short VDF sequences are responsible for the crystal fraction. Therefore, it is not unlikely that different polymorphs may have been formed also in the most "diluted" samples of the present series. Indeed, the X-ray diffraction pattern shows a significant peak at $2\theta = 12°$ only in the samples with 60 and 80 wt % IL (Figure 5 and the text below). More detailed studies, such as temperature dependent X-ray diffraction, could confirm this presumption but this is out of the scope of the present manuscript.

Membrane Structural Properties by X-ray Diffraction Studies. The wide-angle X-ray diffraction patterns of the IL gel membranes and the reference membrane of pure polymer are displayed in Figure 5. The main diffraction peaks are listed in Table 1. The diffraction patterns confirm the general trend of decreasing crystallinity with increasing IL content observed by DSC analysis. In all samples one of the strongest peaks is located at $2\theta = 20°$. The diffraction

pattern of the pure polymer shows some remarkable similarities with that of PVDF, which has two intermediate peaks close together at $2\theta = 18$ and 18.5°, related to the (100) plane and the (020) plane of the α-polymorph, a very strong peak at 20° related to the (110) plane of the α-polymorph, and finally another moderate peak at 27°, due to the (021) plane of the α-polymorph. Upon addition of the IL, the peaks around 18 degrees and 27 degrees disappear completely and the peak at 20° shifts to a slightly higher value. This is the typical position for the (101) plane of the γ-polymorph of PVDF. The only significant novel peak formed at higher IL content appears in the samples with 60% and 80% of IL at ca. 13°, corresponding to a *d*-spacing of 6.78 Å. Its origin is not clear, but given the low polymer concentration, it should presumably involve the IL itself. In these two samples also the DSC first heating run shows a distinct melting peak which is absent in the other samples.

The VDF/HFP ratio in the polymer is approximately 4:1 and statistically VDF sequences with an average of 4 monomeric units should be present, The signals are not sufficiently resolved for a positive identification of the crystal structure but from the low HFP content and the above evaluation it seems likely that short VDF sequences in the copolymer are responsible for a PVDF-like crystal phase and that the presence of the IL favors the formation of one polymorph rather than the other, in the present case probably γ instead of α. The effect of solvents or additives on the polymorph of solution-cast PVDF films is well-known.[26] Also the melting enthalpy of our copolymer (42 J/g) is quite close to that of PVDF (ca. 50 J/g in the second heating run[27]), justifying the hypothesis of a PVDF-like crystal phase.

Table 1. Diffraction Angles (2θ) of the Main Diffraction Peaks of the IL Gel Membranes with the Corresponding Interplanar Distances (*d*-Spacing)

	IL content (wt %)					
diffraction angle, 2θ (deg)	0%	20%	40%	60%	80%	*d*-spacing (Å)
13.0			~	+	+	6.78
17.8	++	~				4.97
20	+++	+++	+++	++	++	4.43
27.1	++					3.28
36	+	++	~	~	~	2.49
38.9	+++					2.32
39.6			++	~	~	2.27
40.9		+				2.20
42.1	+		~			2.14
56	~	~	~			1.64

Mechanical Properties. All membranes were obtained as flexible dense films with sufficient mechanical resistance to be handled without difficulties. The tensile tests were performed on small strips of the films and the results are given in Figure 6 as a function of the ionic liquid content. The ionic liquid has a very strong plasticizing effect on the polymer, causing already at only 20 wt % of IL a decrease of the elastic modulus of an order of magnitude. This is also due to the decrease in crystallinity compared to the neat polymer, as confirmed by DSC. At the same time the break strength of the polymer decreases as a result of the incorporation of the IL. With further increasing IL content both the Young's modulus and the break strength decrease to about 3 and 2 MPa, respectively.

In contrast, the maximum deformation first increases with increasing IL content because of the reduced rigidity and the increased flexibility of the plasticized polymer, and then it rapidly decreases again above 40% of IL, when the gel becomes too weak to undergo a strong plastic deformation. At high IL content, the polymer is more diluted. Under these conditions there is less overlap of the polymer coils in solution and as a consequence the intrachain crystallization becomes relatively more important than interchain crystallization. The latter is responsible for the formation of the physically cross-linked network, and as a consequence the sample loses its mechanical strength and its elasticity.

Gas Transport Properties. The presence of the ionic liquid strongly affects the transport properties of the polymer, but up to about 60 wt % of ionic liquid the membranes still behave more as a glassy polymer rather than as a rubbery polymer. Thus, as the IL content in membrane samples rises, the permeability of all gases investigated increases dramatically (Figure 7). However, the less permeable species (nitrogen and methane) and the most soluble carbon dioxide increase their permeation rate much more than small molecules like helium and hydrogen. Indeed, due to its very stiff nature and the relatively high crystallinity, the neat polymer behaves as a barrier material and its selectivity is mainly determined by its size sieving properties. With increasing IL content the samples become more flexible and this favors the transport of the originally slow species, such as methane and nitrogen, as well as the species with high solubility, such as CO_2. The much higher solubility of CO_2 in comparison with N_2 and H_2 determines the difference in the absolute value of

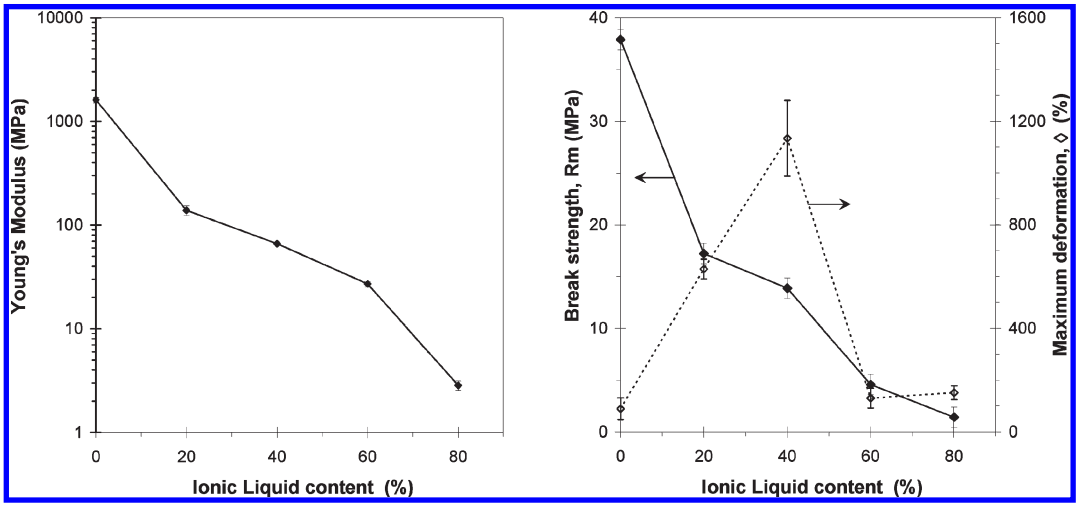

Figure 6. Young's modulus, *E* (left) and the maximum break strength, R_m, and maximum deformation, ε (right), as a function of the IL content.

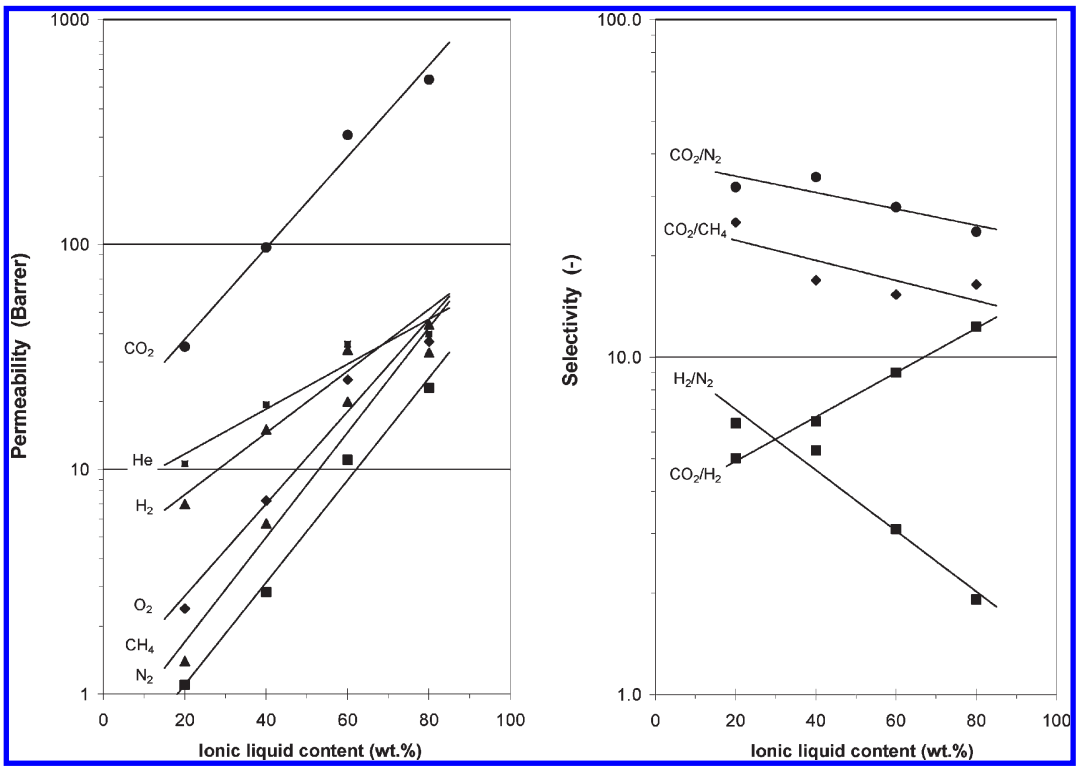

Figure 7. Permeability of six permanent gases as a function of the IL content (left) and corresponding selectivity between selected gas pairs (right). Lines are plotted as a guide to the eye.

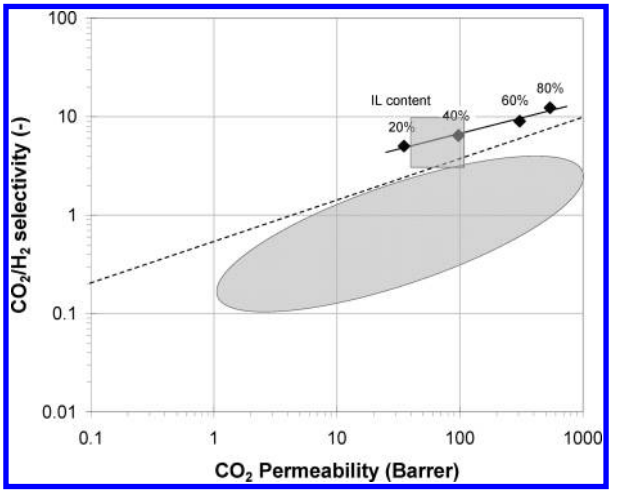

Figure 8. Robeson diagram for the gas pair CO_2/H_2 indicating the experimental points of the present work (♦). The approximate range for common homopolymers (ellipse) and for poly(ethylene glycol) and poly(propylene glycol) derivatives (square), adapted from Patel et al.,[29] are indicated as a reference.

the permeability but does not influence to a large extent the trend as a function of the IL content.

As a consequence the CO_2/N_2 and the CO_2/CH_4 selectivity values undergo only a slight decrease, while the H_2/N_2 selectivity decreases rather strongly with increasing IL content (Figure 7).

On the contrary, as the IL concentration rises, the CO_2/H_2 selectivity shows a remarkable increase, because of the significantly higher positive effect of the IL on the CO_2 permeability than on the hydrogen permeability. The relatively high CO_2 permeability is probably an effect of the affinity of CO_2 for the ionic liquid, and thus of the high solubility of this gas in the membrane. If this is generally applicable, then the presented type of membranes can be successfully used in the separation of those mixtures where species with a significantly different affinity for the ionic liquid are present.

Membranes with such a large CO_2/H_2 selectivity are quite uncommon because hydrogen is usually the faster permeating species. Indeed, in his famous diagrams, Robeson represents the permeation data for the CO_2 and H_2 gas pair as the H_2/CO_2 selectivity against the H_2 permeability.[28] Thus, whereas one usually searches for membranes with a high H_2/CO_2 selectivity, the present membranes behave in the opposite way and might be interesting for those applications where CO_2 must be removed from a hydrogen stream and where hydrogen should remain at high pressure. An alternative Robeson diagram of the CO_2/H_2 selectivity against the CO_2 permeability was presented by Patel et al.[29] (Figure 8). The increase of the upper bound line in this diagram corresponds with the trend in our own experimental data. It is interesting to note that all our data are significantly above the general trend in the data, indicating that IL gel membranes are indeed promising candidates for the given separation.

Conclusions

The fluoroelastomeric polymer p(VDF-HFP) forms stable gels in the ionic liquid [EMIM][TFSI], enabling the successful preparation of resistant free-standing membranes by solution casting of the polymer/ionic liquid mixture, followed by controlled solvent evaporation. The membranes consist of a thermoreversible polymeric gel in which crystallization of p(VDF-HFP) is responsible for the network structure, as supported by DSC and X-ray diffraction analysis. The polymer shows a good compatibility with the IL and may swell up to 30% at room temperature, while it becomes soluble at 90 °C or higher, depending on the concentration of IL.

The presence of IL in the polymer causes a decrease of the elastic modulus of several orders of magnitude and a significant

reduction of the break strength over the entire concentration range. On the other hand, the maximum deformation initially increases to over 1000% and then decreases for an IL content above 40%. This is due to a compromise between the increased elasticity of the gel (lower Young's modulus), leading to higher elongations, and the reduced break strength, leading to lower elongations.

DSC analysis shows a strong decrease of the polymer melting point in the gel as a function of the IL content and a decrease of the overall melting enthalpy. However, normalized for the polymer concentration, the melting enthalpy tends to increase at the higher IL concentrations, presumably due to more efficient chain folding as a result of the lower viscosity and higher mobility of the polymer chains in the IL solution.

The gas permeability strongly rises with the IL concentration and the transport of larger and more condensable species is favored over that of the smaller molecules. The separation thus changes from a diffusion-controlled process to a solubility-controlled one. The CO_2/H_2 selectivity is unusually high for this reason, offering perspectives for application of these membranes in environments where carbon dioxide must be separated from hydrogen while the latter remains at high pressure.

Acknowledgment. This research was supported by the CNR-CAS bilateral agreement 2010-2012 (Novel composite membranes containing selected ionic liquids and polymers for gas and vapour separations). The authors are also thankful for the financial support of the Czech Ministry of Education, Sports and Youth MSM (Grant No. 6046137307) and of the Czech Science Foundation (Grant No. P106/10/1194) and the Grant Agency of the Czech Republic (Grant No. 203/08/0465). Alessio Fuoco, Fabio Bazzarelli, and Paola Bernardo are gratefully acknowledged for their assistance in the tensile tests and in the gas permeation measurements. Alena Randová and Lidmila Bartovská are also gratefully acknowledged for their assistance in the swelling measurements.

References and Notes

(1) Freemantle, M. New Horizons for Ionic Liquids. *Chem. Eng. News* **2001**, 21–25.
(2) Fadeev, A. G.; Meagher, M. M. Opportunities for ionic liquids in recovery of biofuels. *Chem. Commun.* **2001**, 295–296.
(3) Kohoutová, M.; Sikora, A.; Hovorka, Š.; Randová, A.; Schauer, J.; Tišma, M.; Setničková, K.; Guernik, S.; Greenspoon, N.; Izák, P. Influence of ionic liquid content on properties of dense polymer membranes. *Eur. Polym. J.* **2009**, *45*, 813–819.
(4) Izák, P.; Schwarz, K.; Ruth, W.; Bahl, H.; Dyson, P. J.; Kragl, U. Increased productivity of Clostridium acetobutylicum fermentation of acetone, butanol, and ethanol by pervaporation through supported ionic liquid membrane. *Appl. Microbiol. Biotechnol.* **2008**, *78*, 597–602.
(5) Scovazzo, P. Determination of the upper limits, benchmarks and critical properties for gas separations using stabilized room temperature ionic liquid membranes (SILMs) for the purpose of guiding future research. *J. Membr. Sci.* **2009**, *343*, 199–211.
(6) Izák, P.; Friess, K.; Šípek, M. Pervaporation and Permeation Taking Advantage of Ionic Liquids. in *Handbook of Membrane Research: Properties, Performance and Applications*; Gorley, S. V., Ed.; Nova Science Publishers: Hauppauge, NY, 2009; Chapter 12.
(7) Branco, L. C.; Crespo, J. G.; Afonso, C. A. M. Studies on the Selective Transport of Organic Compounds by Using Ionic Liquids as Novel Supported Liquid Membranes. *Chem.—Eur. J.* **2002**, *8*, 3865–3871.
(8) Bara, J. E.; Lessmann, S.; Gabriel, C. J.; Hatakeyama, E. S.; Noble, R. D.; Gin, D. L. Synthesis and performance of polymerizable room temperature ionic liquids as gas separation membranes. *Ind. Eng. Chem. Res.* **2007**, *46*, 5397–5404.
(9) Bara, J. E.; Hatakeyama, S. E.; Gin, D. L.; Noble, R. D. Improving CO_2 permeability in polymerized room-temperature ionic liquid gas separation membranes through the formation of a solid composite with a room-temperature ionic liquid. *Polym. Adv. Technol.* **2008**, *19*, 1415–1420.
(10) Hiltner, A. Gelation Properties of Polymer Solutions. In *Polymer Handbook*, 4th ed.; Brandrup, J., Immergut, E. H., Grulke, E. A., Eds.; John Wiley & Sons: New York, 1999; Chapter 7.
(11) Harner, J. M.; Hoagland, D. A. Thermoreversible gelation of an ionic liquid by crystallization of a dissolved polymer. *J. Phys. Chem. B* **2010**, *114*, 3411–3418.
(12) He, Y.; Lodge, T. P. Thermoreversible ion gels with tunable melting temperatures from triblock and pentablock copolymers. *Macromolecules* **2008**, *41*, 167–174.
(13) Kawauchi, T.; Kumaki, J.; Okoshi, K.; Yashima, E. Stereocomplex formation of isotactic and syndiotactic poly(methyl methacrylate)s in ionic liquids leading to thermoreversible ion gels. *Macromolecules* **2005**, *38*, 9155–9160.
(14) Krull, F. F.; Fritmann, C.; Melin, T. Liquid Membranes for Gas/Vapor Separations. *J. Membr. Sci.* **2008**, *325*, 509–519.
(15) Mehnert, C. P. Supported Ionic Liquid Phases. *Chem.—Eur. J.* **2005**, *11*, 50–56.
(16) Kim, H. J.; Nah, S.S..; Min., B. R. A new technique for preparation of PDMS pervaporation membrane for VOC removal. *Adv. Env. Res.* **2002**, *6*, 255–264.
(17) Majumdar, S.; Bhaumik, D.; Sirkar, K. K. Performance of commercial-size plasmapolymerized PDMS-coated hollow fiber modules in removing VOCs from N_2/air. *J. Membr. Sci.* **2003**, *214*, 323–330.
(18) Sohn, W. I.; Ryu, D. H.; Oh, S. J.; Koo, J. K. A study on the development of composite membranes for the separation of organic vapors. *J. Membr. Sci.* **2000**, *175*, 163–170.
(19) Yampolskii, Y.; Pinnau, I.; Freeman, B. *Materials Science of Membranes for Gas and Vapor Separation*: John Wiley & Sons: Chichester, England, 2006.
(20) Šindelář, V.; Sysel, P.; Hynek, V.; Friess, K.; Šípek, M.; Castaneda, N. Transport of Gases and Organic Vapors Through Membrane Made of Poly(amide-imide)s Crosslinked With Poly(ethyleneadipate). *Collect. Chech Chem. Commun.* **2001**, *66*, 533–540.
(21) Guizard, C.; Boutevin, B.; Guida, F.; Ratsimihety, A.; Amblard, P.; Lasere, J. C.; Naiglin, S. VOC Vapor Transport Properties of New Membranes Based on Cross-linked Fluorinated Elastomers. *Sep. Purif. Technol.* **2001**, *22*, 23–30.
(22) Obuskovic, G.; Majumdar, S.; Sirkar, K. K. Highly VOC-selective hollow fiber membranes for separation by vapor permeation. *J. Membr. Sci.* **2003**, *217*, 99–116.
(23) (a) Clarizia, G.; Algieri, C.; Drioli, E. Filler-polymer combination: a route to modify gas transport properties of a polymeric membrane. *Polymer* **2004**, *45*, 5671–5681. (b) Macchione, M.; Jansen, J. C.; De Luca, G.; Tocci, E.; Longeri, M.; Drioli, E. Experimental analysis and simulation of the gas transport in dense Hyflon AD60X membranes. Influence of residual solvent. *Polymer* **2007**, *48*, 2619–2635.
(24) Jansen, J. C.; Friess, K.; Drioli, E. Organic vapour transport in glassy perfluoropolymer membranes. A simple semi-quantitative approach to analyze clustering phenomena by time lag measurements, *J. Membr. Sci.* **2011**, *367*, 141−151.
(25) Lovinger, A. J. Poly(vinylidene fluoride). In *Developments in crystalline polymers-1*; Bassett, D. C., Ed.; Applied Science Publishers: London, England, 1982; pp 195−273.
(26) Benz, M.; Euler, W. B. Determination of the crystalline phases of poly(vinylidene fluoride) under different preparation conditions using differential scanning calorimetry and infrared spectroscopy. *J. Appl. Polym. Sci.* **2003**, *89*, 1093–1100.
(27) Choi, S.-H.; Tasselli, F.; Jansen, J. C.; Barbieri, G.; Drioli, E. Effect of the preparation conditions on the formation of asymmetric poly(vinylidene fluoride) hollow fibre membranes with a dense skin. *Eur. Polym. J.* **2010**, *46*, 1713–1725.
(28) Robeson, L. M. The upper bound revisited. *J. Membr. Sci.* **2008**, *320*, 390–400.
(29) Patel, N. P.; Hunt, M. A.; Lin-Gibson, S.; Bencherif, S.; Spontak, R. J. Tunable CO_2 transport through mixed polyether membranes. *J. Membr. Sci.* **2005**, *251*, 51–57.